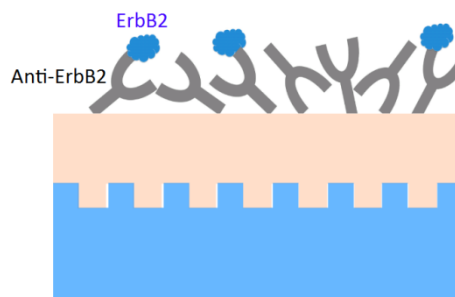
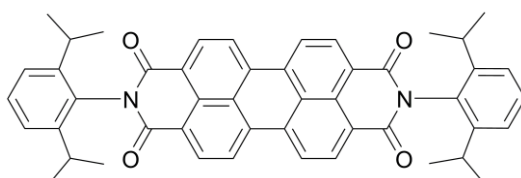
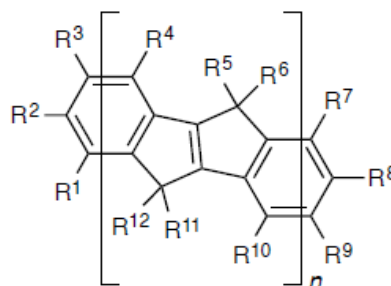
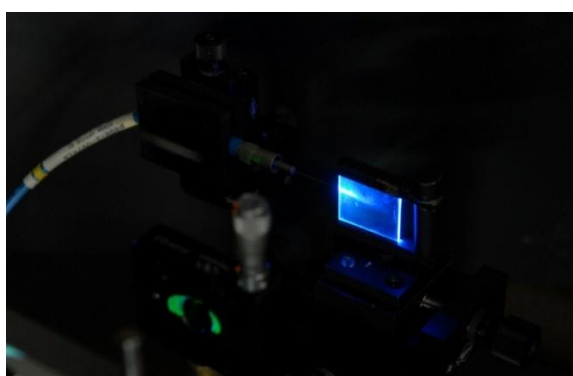




Universitat d'Alacant  
Universidad de Alicante

# High performance thin film organic lasers for sensing applications



**MARTA MORALES VIDAL**

**Tesis doctoral**

Alicante, Diciembre de 2015



Universitat d'Alacant  
Universidad de Alicante

DEPARTAMENTO DE FÍSICA APLICADA

FACULTAD DE CIENCIAS

# High performance thin film organic lasers for sensing applications

**MARTA MORALES VIDAL**

Tesis presentada para aspirar al grado de

DOCTORA POR LA UNIVERSIDAD DE ALICANTE

MENCIÓN DE DOCTORA INTERNACIONAL

DOCTORADO EN NANOCIENCIA Y NANOTECNOLOGÍA

Dirigida por:

**María Ángeles Díaz García**

Catedrática de Universidad (Área: Física de la materia condensada)

This PhD thesis has been supported by the Spanish Government, in projects: MAT2008-06648-C02-01 and MAT-2011-28167-C02-01, where Marta Morales is funded under a FPI grant (BES-2009-020747).



A mis abuelos y abuelas, en especial a Salvadora, quién terminó de escribir las páginas de su historia durante mi estancia en St. Andrews.



## Agradecimientos

Terminando el manuscrito donde intento plasmar las investigaciones realizadas durante mi periodo de doctorado, llega el momento de agradecer a todas las personas e instituciones que han hecho posible que llegara este momento.

En primer lugar, y como no podía ser de otra manera, quiero a agradecer a mi tutora María Díaz-García, su confianza depositada en mí para estudiar unos novedosos materiales láser con los que hemos conseguido grandes éxitos. También por permitirme participar en la prometedora línea de investigación relacionada con los biosensores. Su entusiasmo por la investigación, su trabajo incansable y sus sabios consejos, me han ayudado a seguir adelante. Pedro Boj dispuesto siempre para trabajar, ha sido una pieza clave en los experimentos. Sin su alto grado de perseverancia no se habría llegado a conseguir estudios tan elaborados como algunos de los que se presentan en esta tesis. El equipo compuesto por Moisés Villalvilla y José Antonio Quintana se caracteriza por su minuciosa perfección y por tratar de encontrar siempre la explicación que hay detrás de los resultados de laboratorio. Gracias por contribuir en diversos estudios y por estar encantados de resolverme dudas a cualquier hora. Eva Calzado, la primera doctora formada en el grupo, siempre ha estado dispuesta a echarme una mano, escucharme y comprenderme. Por último, no debo olvidar a los doctores Víctor Navarro y Manuel G. Ramírez por enseñarme cómo funcionaba el laboratorio en la primera etapa de mi tesis.

Por un lado, desde la Universidad de Málaga, Juan Casado nos propuso, con acierto, evaluar las características ópticas de unos nuevos materiales activos. En este sentido el grupo del profesor Nakamura, en la Universidad de Tokio, nos han proporcionado toda una familia de materiales activos láser gracias a los cuales hemos podido publicar un artículo de alto impacto y una patente. Por otro lado, hemos trabajado con Tekniker (País Vasco), quienes nos han proporcionado redes grabadas por nanoimpresión de alta calidad, útiles para realizar nuestros dispositivos láser. En especial agradezco a Santos y Aritz su colaboración para la publicación de los trabajos relacionados con sensores. Con Aritz he tenido la suerte de trabajar directamente en la Universidad de Alicante, y aprender de él acerca de la funcionalización del sensor que diseñamos.

Durante la última etapa de mi tesis, tuve la suerte de poder trabajar en la prestigiosa Universidad de St. Andrews (Escocia) donde los profesores Ifor Samuel y Graham Turnbull me acogieron muy amablemente, a la vez que se interesaron frecuentemente por el estado de mis investigaciones. Además, durante esta estancia, debo agradecer a Guy Whitworth por ayudarme y participar en los experimentos. Y en general, a todos los compañeros que tuve allí e hicieron me sintiera como en casa.

La realización de esta tesis ha estado financiada por la Secretaría de Estado de Investigación mediante los proyectos MAT2008-06648-C02-01 y MAT-2011-28167-C02-01 y particularmente por la concesión de la beca FPI, BES-2009-020747. Gracias a la concesión de esta beca pude iniciar mis estudios en el Máster de Nanociencia y

Nanotecnología Molecular y posteriormente llevar a cabo mis estudios de doctorado. Todos estos estudios se han desarrollado en el Departamento de Física Aplicada de la Universidad de Alicante al que debo agradecer permitirme usar su infraestructura, así como facilitarme materiales y servicios. Dentro de éste me gustaría agradecer a todos los profesores del departamento su familiaridad y profesionalidad. Gracias también por la disponibilidad y el buen hacer de los informáticos y de los responsables de la administración.

Agradezco al Instituto Universitario de Materiales de la Universidad de Alicante haber gestionado los proyectos anteriormente comentados y también haber subvencionado parte de estos estudios. En este sentido Toya me ha ayudado eficientemente siempre cuando he necesitado cualquier trámite. También Toñi desde Becas y Convocatorias Públicas ha estado disponible para ayudar eficientemente en todos los trámites de la beca FPI.

Pero no menos agradecimientos se merecen los estudiantes de doctorado y post-docs que han llenado el Departamento de Física Aplicada de alegría, humanidad y juventud: Danielle, Dani, Carmen, Miguel, Bernat, Jesús, M<sup>a</sup> José, Raúl, Taner... habéis sido un gran apoyo y habéis conseguido que venir a la Universidad significara encontrarte con gente de la que siempre podías aprender. Gracias M<sup>a</sup> José por ser además de compañera, amiga, no olvido tu gesto de salvación cuando más lo necesitaba.

Creo conveniente nombrar a las doctoras Ana y M<sup>a</sup> José y a los doctores Fran y Carlos por intercambiar vivencias de este mundillo de la universidad, también a Lidia por echarme una mano cuando lo necesitaba. Tampoco puedo olvidarme de mi familia y en especial de mis padres, por formarme como persona, por enseñarme los valores de trabajo y sacrificio, pero sobre todo, por estar siempre ahí. Y es inevitable que no nombre a mi apoyo constante en los buenos y malos momentos, a esa persona que me ha proporcionado consejos y reflexión ante las dificultades en este largo camino, Jesús Fernández. Gracias por creer siempre en mis posibilidades y sobre todo apoyarme tanto en la recta final de mi tesis.

Mi gran compañero de fatigas, Miguel, me ha ayudado a encontrar una frase para comenzar esta tesis:

*“Les étoiles sont éclairées pour que chacun puisse un jour retrouver la sienne”*

Antoine de Saint-Exupéry

*Le Petit Prince*

Esta frase de la novela de *El principito* traducida al castellano sería:

*“Me pregunto si las estrellas se iluminan con el fin de que algún día, cada uno pueda encontrar la suya”*

In English:

*“I wonder if the stars are lit up so that each one of us can find her own star again.”*





# ÍNDICE

---

Abbreviation list	XIII
Symbol list	XVII
Introduction	XXI

## I. PHYSICS FUNDAMENTALS AND BACKGROUND

<b>CHAPTER 1. Photophysic fundamentals</b>	<b>3</b>
<b>1.1. Principles of a laser</b> .....	<b>4</b>
1.1.1. Stimulated and spontaneous radiation processes.....	4
1.1.2. Essential elements of a laser.....	5
1.1.3. Threshold gain condition.....	6
1.1.4. Laser output-beam properties.....	6
1.1.5. Laser cavity or resonator: laser modes.....	7
<b>1.2. Amplified emission without resonant cavity: amplified     spontaneous emission (ASE)</b> .....	<b>9</b>
<b>1.3. Waveguide description</b> .....	<b>11</b>
<b>1.4. Types of laser resonators</b> .....	<b>13</b>
<b>1.5. Distributed feedback (DFB) lasers</b> .....	<b>14</b>
<b>CHAPTER 2. DFB lasers for sensing</b>	<b>17</b>
<b>2.1. Introduction</b> .....	<b>18</b>
<b>2.2. Overview of refractive index sensors</b> .....	<b>19</b>
<b>2.3. DFB lasers as bulk refractive index sensors</b> .....	<b>21</b>

<b>2.4. DFB lasers as biosensors.....</b>	<b>22</b>
2.4.1. Cell-assays.....	22
2.4.2. Determination of sensor parameters in a DFB biosensor.....	23
2.4.3. DFB biosensors state-of-the-art.....	23
<b>2.5. DFB lasers to monitor solvent extraction in annealed polymer     films.....</b>	<b>24</b>

## **CHAPTER 3. Gain materials used in organic DFB lasers      27**

<b>3.1. Introduction.....</b>	<b>28</b>
<b>3.2. Organic gain media typically used in organic DFB lasers.....</b>	<b>29</b>
3.2.1. Organic semiconductors versus dye-doped polymers.....	31
3.2.2. Emission wavelength tunability.....	35
<b>3.3. Organic gain media used in DFB sensors.....</b>	<b>36</b>

## **II. EXPERIMENTAL METHODS**

### **CHAPTER 4. Experimental procedures      41**

<b>4.1. Preparation of laser devices.....</b>	<b>42</b>
4.1.1. Spin coating process for deposition of active organic thin films.....	42
4.1.2. Thermal treatments.....	44
4.1.3. DFB fabrication.....	45
<b>4.2. Characterization of standard optical properties.....</b>	<b>48</b>
4.2.1. Absorption and film thickness measurements.....	48

4.2.2. Photoluminescence (PL) measurements, including PL Quantum Yield (PLQY).....	50
4.2.3. Refractive index determination (Abelès method).....	53
<b>4.3. Amplified spontaneous emission characterization.....</b>	<b>53</b>
4.3.1. Setup.....	53
4.3.2. ASE parameters determination.....	56
<b>4.4. Distributed feedback laser characterization.....</b>	<b>58</b>
4.4.1. Setup.....	58
4.4.2. DFB laser parameters determination.....	59
<b>4.5. DFB laser used as sensor.....</b>	<b>59</b>
4.5.1. Setup.....	59
4.5.2. DFB sensor parameters determination.....	60
4.5.3. Biosensor functionalization.....	61
<b>4.6. Experimental procedures in the University of St. Andrews.....</b>	<b>62</b>
4.6.1. Device preparation.....	62
4.6.2. Optical characterization.....	62

### **III. RESULTS**

#### **CHAPTER 5. DFB lasers for sensing applications 67**

##### **5.1. Introduction..... 68**

##### **5.2. DFB laser as bulk refractive index sensor..... 68**

    5.2.1. High sensitivity sensors based on very thin active films..... 68

    5.2.2. DFB sensors with thick films and the use of TE<sub>1</sub> mode..... 71

5.2.3. Influence of film thickness on the ASE and DFB properties.....	72
5.2.4. Two-layer DFB laser (TiO <sub>2</sub> /PDI-O doped PS over resonator).....	75
<b>5.3. DFB laser as biosensor.....</b>	<b>77</b>
5.3.1 Biosensing capabilities.....	78
5.3.2 ErbB2 immunoassay.....	79
<b>5.4. DFB laser to monitor solvent extraction upon thermal annealing.....</b>	<b>80</b>
5.4.1. Solvent loss and wavelength shift as a function of annealing time..	80
5.4.2. DFB sensor sensitivity.....	82
<b>5.5. Conclusions.....</b>	<b>83</b>
<b>CHAPTER 6. Carbon-bridged oligo(<i>p</i>-phenylenevinylene)s (COPVs) as novel laser materials</b>	<b>87</b>
<b>6.1 Introduction.....</b>	<b>88</b>
<b>6.2 Absorption, PL and ASE properties of COPV<sub><i>n</i></sub> dispersed in polymer films.....</b>	<b>90</b>
6.2.1 Absorption, PL and ASE spectra of COPV <sub><i>n</i></sub> dispersed in polystyrene films.....	90
6.2.2 ASE threshold, PLQY and gain coefficient.....	92
6.2.3 ASE photostability .....	97
6.2.4 Effect of replacing polystyrene by poly(methyl methacrylate).....	100
<b>6.3 DFB lasers based on COPV<sub><i>n</i></sub>-based active films.....</b>	<b>101</b>
6.3.1 DFB spectra.....	101
6.3.2 Threshold and photostability.....	103
6.3.3 DFB lasers with resonators on top layer over the active film.....	107

<b>6.4 Other COPV compounds.....</b>	<b>110</b>
6.4.1 COPV-IPR.....	110
6.4.2 Poly-COPV1.....	113
<b>6.5. Conclusions.....</b>	<b>115</b>
<b>CHAPTER 7. General conclusions and future research</b>	<b>119</b>
<b>Resumen/Spanish abstract</b>	<b>121</b>
<b>Publications and conference contributions</b>	<b>137</b>
A. Publications on the scope of the thesis.....	137
B. Patents.....	138
C. Other publications.....	138
D. Conference contributions.....	138
<b>References</b>	<b>141</b>



## Abbreviation list

ABS	Absorbance
ADS223YE	Fluorene co-polymer
Alq <sub>3</sub>	Tris(8-hydroxyquinoline) aluminum
Anti-ErbB2	Anti-epidermal growth factor receptor 2 monoclonal antibodies
ASE	Amplified spontaneous emission
b.p.	Boiling point
BBEHP-PPV	Poly(2,5-bis(2',5'-bis(2''-ethylhexyloxy)phenyl)- p -phenylenevinylene)
BN-PFO	Poly[9,9-dioctylfluorene-co-9,9-di(4-methoxy-phenyl)fluorene
b-PDI-1	Bay-substituted PDI presenting two sterically hindering diphenylphenoxy groups at the 1,7 positions and ethylpropyl substituents in the imide positions
BSA	Bovine Serum Albumin
C 503	Coumarin 503
CCD	Charge-coupled device
CD	Compact Disc
COPV <sub>n</sub>	Carbon-bridged oligo(p-phenylenevinylene
COPVs	Carbon-bridged phenylenevinylenes
CTMA	Cetyltrimethyl ammonium chloride
DCG	Dichromated gelatine
DCM	4-dicyanomethylene-2-methyl-6-(p-dimethylaminostyryl)-4H-pyran
DCNP	3-(1,1-dicyanoethenyl)-1-phenyl-4,5-dihydro-1H-pyrazole
DFB	Distributed feedback
DNA	Deoxyribonucleic acid
DVD	Digital Video Disc
EBL	Electron beam lithography
ErbB2/ HER2	Epidermal growth factor receptor 2 oncogene



## Abbreviation list

---

F8BT	(Poly[(9,9-dioctylfluorenyl-2,7-diyl)- co -(1,4-benzo-{2,1',3}-thiadiazole)])
F8DP	Poly[9,9-dioctylfluorene-co-9,9-di(4-methoxy-phenyl)]fluorine
FWHM	Full width at half maximum
GC	Gas chromatograph
HEMA	Hydroxyethylmethacrylate
HL	Holographic lithography
IgG	Human immunoglobulin G
LASER	Light Amplification by Stimulated Emission of Radiation
LDS722	Hemicyanine
LEDs	Light Emitting Diodes
LOD	Limit of detection
MASER	Microwave Amplification by Stimulated Emission of Radiation
MEH-PPV	Poly[2-methoxy-5-(2'-ethylhexyloxy)-1,4-phenylene vinylene]
MMA	Methyl methacrylate
MS	Mass spectrometer
Nd:YAG	Neodymium-doped yttrium aluminium garnet
NIL	Nanoimprint lithography
Ormoc.	Ormocomp
OPO	Optical Parametric Oscillator
OS	Organic Semiconductors
OSLs	Organic solid-state lasers
PAZO	Azobenzene-containing polyelectrolyte
PBS	Phosphate-buffered saline
PC	Photonic crystal
PDI	Perylene diimide
PDI-C6	(N,N'-bis(1-hexylheptyl)-perylene-3,4:9,10-bis(dicarboximide))

## Abbreviation list

---

PDI-O	Perylene orange, N,N'-di(2,6-diisopropylphenyl)perylene-3,4:9,10-tetracarboxylic diimide
PF	Polyfluorenes
PF <sub>3</sub> C <sub>z</sub>	Random fluorene/carbazole co-polymer
PL	Photoluminescence
PM	Pyrrromethene
PMMA	Poly(methyl methacrylate)
Polycarb.	Polycarbonate
Poly-COPV1	Carbon-bridged phenylenevinylene polymer
pp	Pump pulses
PPVs	Polyphenylenevinylenes
PS	Polystyrene
PVK	Poly(9-vinylcarbazole)
PWV	Peak wavelength value
Rh	Rhodamine
Rh590	Rhodamine 590
RIU	Refractive index unit
RT-NIL	Room temperature nanoimprint lithography
S50F8:50F5	50% 9,9-dioctylfluorene and 50% 9,9-di(2-methyl)butyl
SERS	Surface-Enhanced Raman Scattering
SiO <sub>2</sub>	Silicon dioxide (obtained by oxidation of a silicon wafer)
SPR	Surface plasmon resonances
SPW	Surface plasmon wave
SRS	Stimulated Raman scattering
T3	Tris(trifluorene)truxene

## Abbreviation list

---

T4	Oligofluorene truxene, hexahexylated truxene core onto which fluorene arms are attached, with each arm consisting of four 9,9- dihexylfluorene units
TD	Thermal Desorption
TE	Transverse electric
TEM	Transverse electromagnetic
TFOLs	Thin Film Organic Lasers
TiO <sub>2</sub>	Titanium dioxide
TM	Transverse magnetic
TMSPMA	3-(trimethoxysilyl)propyl methacrylate
TNF $\alpha$	Tumor necrosis factor alpha
T-NIL	Thermal nanoimprint lithography
UV-NIL	Ultraviolet nanoimprint lithography
VSL	Variable Stripe Length
WGM	Whispering gallery modes
1D	One-dimensional
[2(C <sub>6</sub> H <sub>13</sub> )]	Pyrene-Cored Starburst
Y80F8:20F5	80% 9,9-dioctylfluorene and 20% 9,9-di(2-methyl)butyl

## Symbols list

$A$	Constant related to the cross section for spontaneous emission
$C$	Molar concentration
$c$	Speed of light in vacuum
$d$	Grating depth
$E$	Electric field
$E$	Energy level
$G$	Gain
$g_{\text{net}}$	Net gain coefficient
$H$	Magnetic field
$\hbar$	Planck constant
$h_{\text{cut-off}}$	Thickness below which the mode cannot propagate in the guide
$h_f$	Film thickness
$I$	Irradiance of the beam
$I_{\text{max}}$	Maximum intensity
$I_{\text{min}}$	Minimum intensity
$I_{\text{pump}}$	Pump intensity
$I_{\text{th}}$	Threshold intensity
$k$	Wave number
$k_g$	Gain coefficient
$k_{\text{th}}$	Threshold gain coefficient
$l$	Cell thickness
$L$	Gain length
$L_c$	Coherence length
$l_{\text{ps}}$	Length of the pump stripe
$M_w$	Molecular weight

$n_a$	Air refractive index
$n_c$	Cover layer refractive index
$n_{\text{eff}}$	Effective index
$n_f$	Film refractive index
$n_s$	Substrate refractive index
$q$	Longitudinal mode index, integer number
$R$	Reflectivity
$r$	Sensor resolution
$S_b$	Sensitivity
$t$	Time
$T$	Transmittance
$T_a$	Temperature
$T_g$	Glass transition temperature
$t_p$	Excitation pulse duration
$V$	Visibility
$\alpha$	Absorption coefficient
$\theta$	Angle of incidence with respect to the normal to the interface
$\omega$	Angular velocity
$\beta$	Brewster angle
$\tau_c$	Coherence time
$\theta_c, \theta_s$	Critical angles
$\rho$	Density
$\epsilon_r$	Dielectric constant
$\chi_e$	Electric susceptibility
$\gamma$	Energy losses
$\nu$	Frequency

## Symbols list

---

$\Lambda$	Grating period
$\varepsilon$	Molar extinction coefficient
$\tau_{1/2}$	Photostability halflife determined as the time on the number of pump pulses at which the emitted intensity decays to half of its initial value
$\tau_{1/e}$	Photostability lifetime defined as the time on the number of pump pulses at which the emitted intensity decays to 1/e of its initial value
$\Delta\nu$	Spectral band-width
$\lambda_{\text{Bragg}}$	The resonant wavelength in the cavity that satisfies the Bragg condition
$\lambda$	Wavelength



## Introduction

The first practical **LASER**, demonstrated by Maiman in 1960,<sup>1</sup> has produced a revolution in Science and Technology. Applications using lasers have spread among many areas, such as Research, Medicine, Telecommunications, Material processing, etc. Nowadays, lasers are used in our everyday life, for example they are frequently used in compact disc (CD) and digital video disc (DVD) players, printers and supermarket scanners. Among a wide variety of available lasers, those in which the active medium is organic –the organic lasers – are particularly interesting because thanks to the broad photoluminescence (PL) spectra of organic molecules, they allow tuning the emission color across the whole visible spectrum. Besides, thanks to the chemical versatility offered by chemical synthesis, the material properties can be easily modified.

The first **organic laser** was a liquid dye laser,<sup>2,3</sup> in which the active medium consisted of an organic molecule (a dye) dissolved in a solvent (i.e. ethanol, methanol, hexane, etc.). These systems were commercialized and are used in various applications. However, liquid dye lasers present some limitations: large size, the need of high power pumping sources, difficulties in handling due to the need of recirculating the liquid solution to prevent dye photodegradation, etc. So researchers have pursued for years the development of compact and easy-to-handle organic solid-state lasers (OSLs).<sup>4</sup> Among them, of special importance towards achieving compactness, mechanical flexibility and easy integration with other devices, are those in which the active material is in the form of a thin waveguide film of good optical quality (low propagation losses), conforming the subclass of **Thin Film Organic Lasers (TFOLs)**. Within this subclass, those in which the active film can be prepared by means of solution-based methods, such as spin-coating, printing, etc., are preferred for their prospect of reducing device cost.

In 1996 solid-state lasers based on semiconducting luminescent polymers were reported.<sup>5-8</sup> Since then, **Organic Semiconductors, OS**, (including not only polymers, but also oligomers, dendrimers and small molecules) have been the most widely investigated organic gain media, in most cases in the form of neat active films, because of their prospect for developing electrically driven lasers. Most advances with these materials have focused on decreasing the threshold,<sup>4,9-15</sup> thus, allowing in some cases pumping with very compact sources, such as laser diodes or even with light-emitting diodes (LEDs).<sup>13-15</sup>

Therefore, today, optically-pumped TFOLs constitute a very attractive class of low-cost and mechanically flexible devices. A **distributed feedback (DFB) laser**, consisting of a solution-processable waveguide including a diffractive relief grating, has been a



particularly successful TFOL which has already demonstrated its applicability, at laboratory scale, as tunable sources for spectroscopy (Photometry, Raman and Surface-Enhanced Raman Scattering –SERS-, among others),<sup>16,17</sup> amplifiers for Optical Communications,<sup>9,18</sup> vapor explosive chemical sensors<sup>19</sup> and highly sensitive and possibly specific non-intrusive label-free sensors for drug discovery, biological research, diagnostic tests, food safety, etc.<sup>20-22</sup> For most of these applications, devices based on one-dimensional gratings (1D DFB) operating in the second order of diffraction are preferred because the laser beam is emitted perpendicularly to the film surface and its properties are independent of the excitation beam angle over the sample. Today, one of the major challenges remaining to bring TFOLs to the real market is to find an active material which is simultaneously photostable; efficient as to enable pumping with a compact source, such as a LED; capable of emitting at various colours and processable by low-cost solution-based methods.

Among all these applications, of particular interest for the scope of this thesis is the one in which the DFB laser is used as a **bulk refractive index sensor**. The principle of operation consists in detecting changes in the emission laser wavelength upon deposition of liquids of different refractive index. The sensing performance is typically characterized by the bulk sensitivity,  $S_b$ , defined as the resonance wavelength change per refractive index unit (expressed in nm/RIU). The sensor resolution,  $r$ , which refers to the minimum wavelength shift that can be measured, is also an important parameter. In comparison to other refractive index sensors, organic DFB lasers are very attractive because of their high  $S_b$  and  $r$ ,<sup>21,23,24</sup> simple fabrication and integration with other devices, wavelength tuning capability and small size.

An even more interesting application is to use the organic DFB laser as a **biosensor**. In this case the evanescent wave can detect nanoscale materials by functionalizing the surface of the active film. An important advantage of DFB biosensors, with respect to most other biochemical and cell-based assays, is that no labels are needed to detect the analyte. A label is generally designed to be easily measured by its color or its ability to generate photons at a particular wavelength. It is attached to the analyte, so it indirectly indicates its presence, but it has several drawbacks. For example, it often requires special laboratories which generate large quantities of contaminants reagents. Another problem is that fluorophores degrade quickly over time and by exposure to light. The human epidermal growth factor receptor 2 oncogene, also called **ErbB2 protein** or HER2, is one of the most studied protein molecules in the field of cancer. ErbB2 is overexpressed or amplified in around 15-30% of breast cancer,<sup>25</sup> and in many other types of human malignancies such as ovarian, stomach and lung cancer. Until now, ErbB2 had not been studied as receptor molecule or biomarker in a DFB biosensor.

The procedure used to prepare a TFOL is usually a solution-based method, such as spin-coating, casting, printing, etc. In these methods, most of the solvent from the polymer solution evaporates during the deposition process, but a part of it remains in the film, which would affect the material properties, as well as lead to a lack of reproducibility and stability. The solvent can be eliminated with a proper annealing-thermal treatment and often, techniques such as chromatography and neutron reflectometry have been used to quantify the solvent content.<sup>26-28</sup> However, the dependency on film thickness of the effect of the treatment and the amount of remaining solvent are still a matter of controversy. Along the work of this thesis, the possibility of **monitoring the solvent extraction from a polymer film** subjected to thermal treatments, by means of an organic DFB laser, is demonstrated.

In this context the main **OBJECTIVE** of this thesis is to prepare *high performance TFOLs* and to demonstrate their *capability for sensing*. In the first part, we have prepared DFB sensors based on an active material previously investigated in the group: polystyrene (PS) doped with perylene orange (PDI-O), which has shown a very high photostability and a relatively low threshold. In the second part, we have studied a novel class of active compounds called carbon-bridged phenylenevinylenes (COPVs) which have shown an exceptional performance.

This dissertation consists of three fundamental parts:

An **INTRODUCTION** divided in three chapters. The first one provides a description of the photophysic fundamentals which are behind the most important photonic devices and properties described in this thesis: laser, distributed feedback laser, resonator, waveguide and amplified spontaneous emission (ASE). Secondly, an overview of the usage of DFB lasers for sensing is provided (chapter 2): bulk refractive index sensors, biosensors and solvent extraction monitoring. The third chapter provides a state-of-the-art of organic materials used as gain media in DFB lasers and sensors.

The second part is called **EXPERIMENTAL METHODS** (chapter 4), which is dedicated to explain the experimental procedures used in the University of Alicante and in the University of St. Andrews. All the work has been developed in Alicante, except for the study of a COPV polymer, which was carried out in St. Andrews through a three month stay.

In the third part, the **RESULTS** obtained along this thesis are described. It is composed of two chapters. In the first one, three different applications of DFB sensors based PDI-O-doped PS, are demonstrated (chapter 5). In the second one, we describe results obtained with several derivatives of the novel materials family of COPV compounds (chapter 6), particularly a series of six oligomers (COPV $n$ , with  $n = 1 - 6$ ), where  $n$  is the number of repeating units), two COPV compounds with different substituents attached

to the COPV core (COPV1-IPR and COPV2-IPR), and a COPV polymer (poly-COPV1). The DFB lasers based on these materials have shown an excellent performance simultaneously in the various parameters important for applications. Finally, the most important achievements of the presented work, as well as the future lines of investigation, are summarized in the **CONCLUSIONS AND FUTURE PERSPECTIVES** chapter (chapter 7).

---

# **I. PHYSICS FUNDAMENTALS AND BACKGROUND**

---

**CHAPTER 1. Photophysic fundamentals**

**CHAPTER 2. DFB lasers for sensing**

**CHAPTER 3. Gain materials used in organic DFB lasers**



## **CHAPTER 1. Photophysic fundamentals**

### **1.1. Principles of a laser**

1.1.1. Stimulated and spontaneous radiation processes

1.1.2. Essential elements of a laser

1.1.3. Threshold gain condition

1.1.4. Laser output-beam properties

1.1.5. Laser cavity or resonator: laser modes

### **1.2. Amplified emission without resonant cavity: amplified spontaneous emission (ASE)**

### **1.3. Waveguide description**

### **1.4. Types of laser resonators**

### **1.5. Distributed feedback (DFB) lasers**

## 1.1. Principles of a laser

### 1.1.1. Stimulated and spontaneous radiation processes

Every atom in the periodic table, as well as every molecule or ion has its set of quantum energy levels that can be pumped or excited up into higher energy levels ( $E_2$ ) and also make downward transitions to lower levels ( $E_1$ ), emitting radiation of energy  $\hbar\nu_p = E_2 - E_1$  (Planck-Einstein relation), where  $\hbar$  is known as the Planck constant and  $\nu_p$  is the frequency of a photon. This phenomenon has relevance in the emission of light, so below the various transitions that can occur between the quantum energy levels of an atom (or molecule, or ion) are explained.

When we study the coupling of an atom (or molecule, or ion) to a monochromatic light wave, three different radiation processes can be identified: stimulated absorption, stimulated emission and spontaneous emission:<sup>29</sup>

- (I) Stimulated absorption only takes place if there is an applied external field, generally associated to an optical beam, in which an atom is promoted from the ground state to the excited state.
- (II) Stimulated emission takes place when an atom in the excited state decays to the ground state because of the incidence of a photon with energy similar to the difference between states. The emitted photons have very similar phase and energy to the external photon which stimulated them.
- (III) Spontaneous emission is produced when an atom in the excited state decays to the ground state. This process is incoherent or noisy-like.

Any source of light, including the laser, emits light when excited atoms drop to lower states. But for laser action to occur, the pumping process must produce not only excited atoms, but also a condition of population inversion. To achieve it, metaestable states are needed, in which the atom would stay in for long times, if there are not outside influences, such as collisions or certain light waves passing by. Once most molecules are in metaestable states, the population of states is said to be inverted.<sup>30</sup> For this reason, it is impossible to obtain inversion by optically exciting a two-level system. In a system with four states, a dynamic equilibrium can be built, generating a stationary inversion between two of the four levels by supplying energy, and so to fulfill the requirement for running a laser. An inversion can be obtained with three levels as well, whereas the four-level system causes a strict separation of the states directly, contributing to the pumping process and the laser process.<sup>29</sup>

## 1.1.2. Essential elements of a laser

The word LASER (Light Amplification by Stimulated Emission of Radiation) has become a well-recognized word in everyday language. It is derived from its predecessor, the maser (MASER: Microwave Amplification by Stimulated Emission of Radiation).<sup>29</sup> In modern usage, the term “light” in the acronym LASER includes electromagnetic radiation of any frequency, not only visible light. However, because the maser was developed first, devices of this sort operating at microwave and radio frequencies are referred to as “masers”.

The essential elements of a laser device are (figure 1.1):

- (I) A gain medium consisting of an appropriate collection of atoms, molecules or ions in which amplification of optical waves occurs by stimulated emission of radiation.
- (II) A pumping process to excite these atoms (molecules, etc.) into higher quantum mechanical energy levels, or excited states. Generally it may be electric or optical pump (the energy is transferred from an external source into the active medium). Optical pumping techniques may be continuous or pulsed, the last one characterized by the pulse duration,  $t_p$ , and the repetition rate,  $\nu$ .
- (III) Suitable optical feedback elements that allow amplifying a beam of radiation in each pass through the active medium, in order to achieve enough distance traveled so that gain exceeds loss. For example, two mirrors between which the active material is placed (laser or resonant cavity).

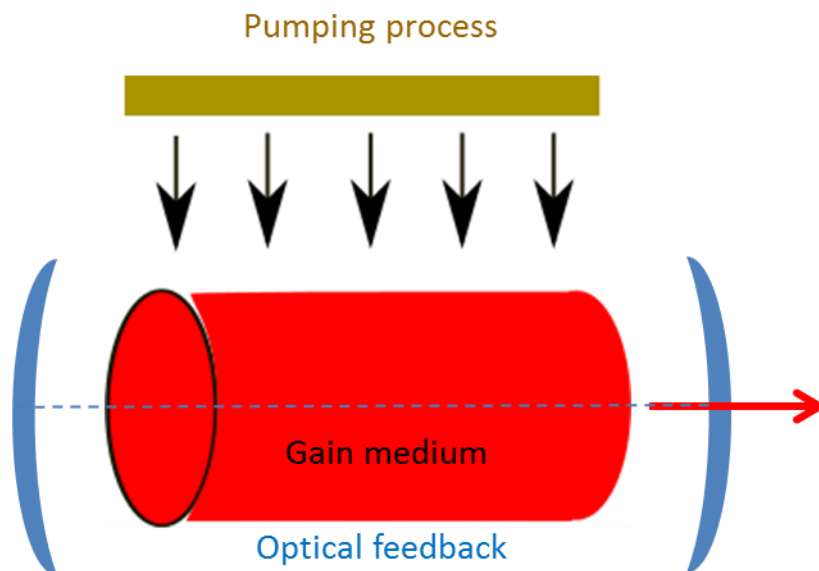


**Figure 1.1.-** Scheme of a standard laser, based on a two-mirror cavity, and its essentials elements.



1.1.3. Threshold gain condition<sup>31-33</sup>

Once population inversion has been generated by pumping energy into the gain medium, laser gain may occur. The process in which a single photon traveling down a laser medium stimulates and excites an atom, which then emits a photon with the same frequency and phase, allows obtaining laser gain. Laser gain (or optical gain) is a measure of how well a medium amplifies photons by stimulated emission. In the ideal case of population inversion, the irradiance of the beam ( $I_0$ ) will increase exponentially ( $I$ ) as a function of the gain length ( $L$ ) and the gain coefficient ( $k_g$ ) as:

$$I(L) = I_0 e^{k_g L} \quad (1.1)$$

In a real situation, for example, in a standard two-mirror laser, as shown in figure 1.1, the emitted laser light will be attenuated by the gain medium as well as by the mirrors, with losses ( $\gamma$ ), causing a reduction in laser gain. The general criterion to obtain lasing is that the stimulated emission should exceed spontaneous emission plus all the losses. In other words, laser oscillation can only sustain in the cavity medium if it attains at least unit gain after a round-trip between mirrors and maintains it overcoming losses inside the cavity. Below this threshold condition is formulated.

Let us consider a laser beam of intensity  $I_0$  which passes through an active medium of length  $L$  homogeneously filling between the space between two mirrors  $M_1$  and  $M_2$  with reflectivities  $R_1$  and  $R_2$ , respectively. The beam of intensity  $I_0$  initiates from the surface of  $M_1$  and attains an intensity  $I_1 = I_0 \exp(k - \gamma)L$  when it reaches the surface of  $M_2$  after traveling a length  $L$ . Then it is reflected in  $M_2$  ( $I'_1 = I_1 R_2$ ) and travels back to  $M_1$ , at which the light intensity becomes  $I_2 = I'_1 \exp(k - \gamma)L$ . Finally,  $I_2$  becomes  $I'_2$  after reflection from  $M_1$  ( $I'_2 = I_2 R_1$ ) to complete a round trip  $I'_2 = I_0 R_1 R_2 \exp 2(k - \gamma)L$ .

Then, by imposing the condition that the gain  $G = I'_2/I_0$  attained in a round-trip should be at least unity to sustain the laser oscillation inside the cavity, the threshold condition would be  $G = R_1 R_2 \exp 2(k - \gamma)L = 1$ , so the expression for the threshold gain coefficient ( $k_{th}$ ) is:

$$k_{th} = \gamma + \frac{1}{2L} \ln \frac{1}{R_1 R_2} \quad (1.2)$$

1.1.4. Laser output-beam properties<sup>31,34</sup>

The output beam from a laser consists of electromagnetic radiation or light that has coherence, property that arises from the classical resonant-cavity properties of the laser resonator, rather than from any of the quantum transition properties of the laser atoms. The term coherence refers not to a property of a signal at a single point in

space and time, but to a relationship between one signal at one point in space and time, and the same or another signal at other points in space and time. Laser beams are often described as being different from ordinary light sources in being temporally or spectrally coherent and spatially coherent. These terms are explained below:

*-Temporal coherence*

The term temporal coherence refers to the correlation between the amplitude and/or the phase of the signal at one time and at earlier or later times. An easy way to measure the temporal coherence of a beam consists in measuring the maximum and minimum intensities ( $I_{\max}$  and  $I_{\min}$  respectively) observed in the interference pattern produced by a Michelson interferometer and then calculating the fringes visibility ( $V$ ) as:

$$V = \frac{I_{\max} - I_{\min}}{I_{\max} + I_{\min}} \quad (1.3)$$

A value of  $V = 1$  implies  $I_{\min} = 0$ , which means perfect temporal coherence.

There are also certain precise mathematical definitions of functions that give the degree of correlation between two signals observed at different points in space and/or time. The coherence time ( $\tau_c$ ) is defined by the delay over which phase or amplitude is predictable. The coherence length ( $L_c$ ) is defined as the distance the wave travels during the time  $\tau_c$ . The temporal coherence and the monochromaticity are related as:

$$\Delta\nu \sim \frac{1}{\tau_c} \quad (1.4)$$

being  $\Delta\nu$  the range of frequencies that a wave contains (spectral band-width).

*-Spatial coherence*

Spatial coherence is the essential prerequisite of the strong directionality of laser beams. Good-quality laser emission is characterized by a very high degree of correlation between the instantaneous amplitudes, and especially between the instantaneous phase angles of the wavefront at any two points across the output beam (spatial coherence).

#### 1.1.5. Laser cavity or resonator: laser modes<sup>31-34</sup>

As we have explained, an essential element of a laser is a feedback structure or optical resonator which allows a beam of light to circulate in a closed path. Therefore, according to eq. (1.1), the effective distance along which light would travel would be large and consequently its gain. In addition, the appearance of longitudinal and transverse modes and directionality properties, are determined by the cavity.

The cavity modes are defined as the standing distributions of the electromagnetic field which obey Maxwell equations and cavity boundary conditions. An optical resonator allows some oscillating transverse electromagnetic (TEM) modes (that means that the electric,  $\mathbf{E}$ , and magnetic,  $\mathbf{H}$ , fields are perpendicular to the propagation direction). It should be distinguished between TE polarization in which  $\mathbf{E}$  is perpendicular to the incident plane, and TM polarization, in which  $\mathbf{H}$  is perpendicular to the incident plane.

In general, the laser cavity is resonant at certain wavelengths,  $\lambda$ , for which the number of waves (standing waves) inside the cavity is an integer number  $q$ . At all other wavelengths the waves are extinguished. These resonant wavelengths are called longitudinal modes and are spaced apart at regular intervals of frequency  $\Delta\nu$ . Assuming that the distance between the cavity mirrors is  $L$ , the condition for a standing wave in the cavity is:

$$q \frac{\lambda}{2} = L \quad (1.5)$$

Taking into account that  $\nu = c/\lambda$ , being  $c$  the speed of light in vacuum:

$$\nu = q \left( \frac{c}{2L} \right) \quad (1.6)$$

These frequencies,  $\nu$ , are known as longitudinal modes while  $q$  is known as the longitudinal mode index. The frequencies of these modes are equally spaced as:

$$\Delta\nu = \nu_{q+1} - \nu_q = \left( \frac{c}{2L} \right) \quad (1.7)$$

The longitudinal modes are related to the monochromaticity and the coherent length ( $L_c$ ) of the laser emission.

Transverse modes are related to the field distribution in a plane perpendicular to the propagation direction of the beam. This distribution determines the spatial coherence. In the simplest description, a laser will oscillate in the form of a more or less uniform, quasi-plane-wave optical beam bouncing back and forth between carefully aligned mirrors at the two ends of the laser resonator. Only waves that are very accurately aligned with the resonator axis will remain within the cavity and be able to oscillate. Hence the beam direction for the oscillating waves will lie very accurately along the cavity axis. Therefore, transverse modes will depend on the cavity mirrors and diaphragms and they will determine the beam directionality.

In many lasers, transverse modes with rectangular symmetry are formed. These modes are designated as  $\text{TEM}_{mn}$ , with  $m$  and  $n$  being the integers referring to the horizontal and vertical orders of the pattern. The  $\text{TEM}_{00}$  is the lowest order or fundamental transverse mode of the laser resonator and has the same form as a Gaussian beam. The pattern has a single lobe, and has a constant phase across the mode. Modes with increasing  $m$  and  $n$  show lobes appearing in the horizontal and vertical directions,

respectively. They are higher-order modes and have a larger spatial extent than the 00 mode.

For a given set of  $m, n$  indexes, it is usual to have some longitudinal modes, with consecutive  $q$  values, that contribute to the optical beam. This fact is because the amplification response of a real active medium occurs in a characteristic frequency range, known as the atomic gain profile. For many lasers, the space between axial modes  $\Delta\nu$  is smaller than the atomic linewidth; and hence there will be several axial-mode cavity resonances within the atomic gain curve or profile. The laser may then oscillate, depending on more complex details, on just the centermost one of these axial modes, or on several axial modes simultaneously.

## **1.2. Amplified emission without resonant cavity: amplified spontaneous emission (ASE)<sup>35-37</sup>**

If population inversion is achieved in a gain medium with three or more levels, it should be able to amplify an incident beam of light. A parameter typically used in the literature to assess the potential of a given material for laser applications is the ASE. ASE appears in systems in which gain is so high that amplification is obtained in a single pass through the material without the need of laser cavity. It is often observed in systems in which light propagates preferentially in a given direction because of the shape of the material (for example when it is a long rod). Due to the high gain, the spontaneous emission is amplified due to the stimulated emission. Since there is no laser cavity, ASE is not true lasing, but a mixture of stimulated emission and spontaneous emission. The main differences between ASE and laser emission are the following:

- (I) The ASE spectrum is narrower than the corresponding fluorescence spectrum but broader than the laser emission spectrum. Typical ASE linewidths are a few nm (i.e. 3-10 nm).
- (II) Properties such as polarization and directionality are less developed in ASE emission, than in laser emission. The output characteristics are somewhere between truly coherent lasing and a completely incoherent emission.
- (III) Absence of resonant laser modes in ASE.

A typical configuration in which ASE occurs is when the active film constitutes a waveguide (figure 1.2). In order to have waveguiding two conditions need to be fulfilled:

- (I) The refractive index of the active film should be larger than that of the substrate and the cover.

- (II) In asymmetric waveguides in which the refractive index of the substrate and the cover are different, the active film thickness should be larger than a certain value, called the cut-off thickness for the propagation of one mode.

More details about these conditions are provided in section 1.3.



**Figure 1.2.-** Waveguide along which light propagates.  $n_c$ : cover layer refractive index;  $n_f$ : film refractive index;  $n_s$ : substrate refractive index ( $n_c < n_f < n_s$ ).

The characterization of the ASE properties is usually carried out by exciting with a beam shaped to a stripe of typically various mm long and around 0.5 mm wide. The light emitted is collected from the edge of the waveguide as a function of the excitation intensity (figure 1.3). If the device is excited above a certain intensity value (called threshold,  $I_{th}$ ) ASE is obtained. The ASE threshold corresponds to the pump intensity at which ASE appears, experimentally evidenced by the observation of a sudden decrease in the emission linewidth, as well as an abrupt enhancement of the output intensity (more details in section 4.3.2).

The ASE emission spectrum narrows at the wavelength at which the net gain is highest. The ASE intensity follows the expression:

$$I(\lambda) = \frac{A(\lambda)I_p}{g_{net}(\lambda)} (e^{g_{net}(\lambda)lps} - 1) \quad (1.8)$$

where  $A$  is a constant related to the cross section for spontaneous emission,  $I_p$  is the pump intensity,  $g_{net}$  is the net gain coefficient, and  $lps$  is the length of the pump stripe. It is possible to determine  $g_{net}$  by measuring the ASE intensity as a function of  $lps$  and fitting data with eq. 1.8 (more details in section 4.3.2).

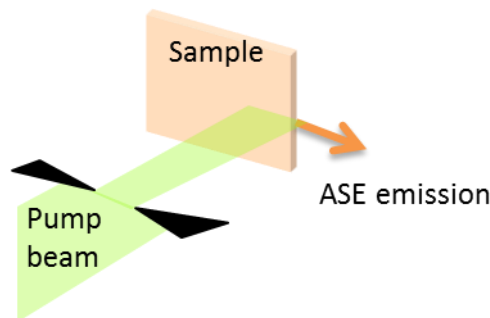


**Figure 1.3.-** Sketch of ASE characterization geometry. Pump (or incident) beam, sample or waveguide and ASE emission.

### 1.3. Waveguide description<sup>38</sup>

An optical waveguide consists of a film in which light is confined and propagates along the film plane (figure 1.4). Light confinement is carried out by successive total reflections in the two interfaces of the guide. Let us consider the case of three media (dielectric, lossless, homogenous and isotropic) with a central layer of refractive index  $n_f$ , surrounded by two layers of indices  $n_s$  and  $n_c$  called the substrate and cover layer respectively. A planar waveguide is characterized by parallel planar boundaries with respect to one direction ( $x$ ), see figure 1.4 and is infinite in extent in the other two directions ( $y$  and  $z$ ).

These waves propagate in the  $z$  direction which their amplitude exponentially decreases in the  $x$  direction. In the optic-ray approach (enough for the purpose of this work) light propagation is carried out by the superposition of several plane waves being propagated in zigzags between the two interfaces, film-cover and film-substrate. The light confinement in such a structure is based on a total reflection phenomenon on the interfaces. Thus, two critical angles  $\theta_c$  and  $\theta_s$  based on Snell Law can be defined as:

$$\sin \theta_c = \frac{n_c}{n_f} \quad (1.9)$$

$$\sin \theta_s = \frac{n_s}{n_f} \quad (1.10)$$

Let's call  $\theta$  the angle of incidence with respect to the normal to the interface (figure 1.4). If  $\theta > \theta_c$ , light is in total reflection on the two interfaces, film-cover and film-substrate, it remains confined between them. These are well confined guided modes.

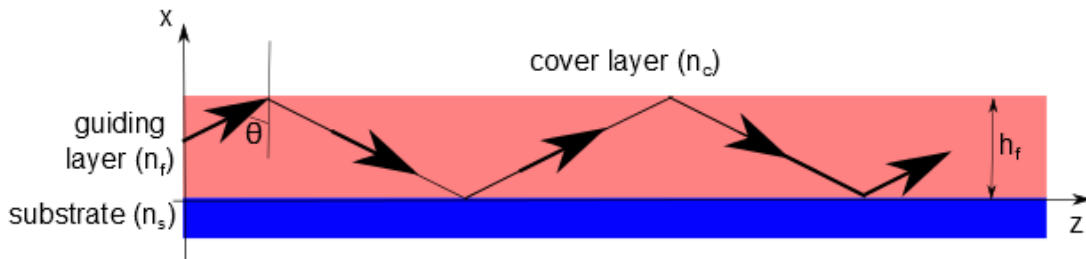


**Figure 1.4.-** Light confined on a film of thickness  $h_f$ .

Let us consider the step index waveguide, where the refractive index remains constant throughout the guide, substrate and cover layer. The phase shift for such a wave is composed by three terms: the phase shift  $\Delta\varphi$ , due to the difference in optical paths (eq. 1.11); and the two phase shifts (according with Fresnel's formulae), which are due to the total reflection on the two interfaces,  $\Phi(n_f, n_c)$  and  $\Phi(n_f, n_s)$ . For the case of TE polarization these shifts are given by eq. 1.12 and 1.13:

$$\Delta\varphi = 2n_f h_f k \cos\theta = \frac{4\pi}{\lambda} n_f h_f \cos\theta \quad (1.11)$$

$$\Phi_{TE(n_f, n_c)} = 2 \operatorname{artg} \left[ \frac{n_f^2 \sin^2 \theta - n_c^2}{n_f^2 - n_f^2 \sin^2 \theta} \right]^{\frac{1}{2}} \quad (1.12)$$

$$\Phi_{TE(n_f, n_s)} = 2 \operatorname{artg} \left[ \frac{n_f^2 \sin^2 \theta - n_s^2}{n_f^2 - n_f^2 \sin^2 \theta} \right]^{\frac{1}{2}} \quad (1.13)$$

where  $k$  is the wave number:  $k = 2\pi/\lambda$ .

In order to maintain light propagation within the guiding layer, it is important that light interferes constructively. For that, the total phase shift should be a multiple of  $2\pi$ . Therefore, we can write the following guided mode dispersion equation as:

$$2n_f h_f k \cos \theta - \Phi_{TE(n, n_c)} - \Phi_{TE(n, n_s)} = 2m\pi \quad (1.14)$$

where  $m$  is an integer  $\geq 0$ .

The eq. 1.14 can be rewritten as a function of the effective index  $n_{\text{eff}}$ , defined as  $n_{\text{eff}} = n_f \sin \theta_m$ . The eq. (1.15) imposes discrete values of  $\theta_m$  related to different values of  $m$ , which determine the set of guided modes for the structure.

$$2kh_f \sqrt{(n_f^2 - n_{\text{eff}}^2)} = \Phi_{TE(n, n_c)} + \Phi_{TE(n, n_s)} + 2m\pi \quad (1.15)$$

$$\Phi_{TE(n, n_c)} = \operatorname{arctg} \left[ \frac{n_f^2 - n_c^2}{n_f^2 - n_{\text{eff}}^2} \right]^{\frac{1}{2}} \quad (1.16)$$

$$\Phi_{TE(n, n_s)} = \operatorname{arctg} \left[ \frac{n_f^2 - n_s^2}{n_f^2 - n_{\text{eff}}^2} \right]^{\frac{1}{2}} \quad (1.17)$$

By inserting the eq. 1.16 and 1.17 in eq. 1.15, we can obtain an expression that provides the  $n_{\text{eff}}$  values as a function of  $n_s$ ,  $n_f$ ,  $n_c$ ,  $h_f$  and  $\lambda$ , as follows:

$$\frac{2\pi}{\lambda} h_f \sqrt{n_f^2 - n_{\text{eff}, m}^2} - \operatorname{arctg} \sqrt{\frac{n_{\text{eff}, m}^2 - n_c^2}{n_f^2 - n_{\text{eff}, m}^2}} - \operatorname{arctg} \sqrt{\frac{n_{\text{eff}, m}^2 - n_s^2}{n_f^2 - n_{\text{eff}, m}^2}} = m\pi \quad (1.18)$$

It should be noticed that the  $n_{\text{eff}}$  value of a given guided mode of order  $m$  increases as film thickness increases.

In an assymmetric waveguide, that is, in which  $n_s \neq n_c$ , the minimum value of effective index which allows waveguiding corresponds to a thickness below which the mode cannot propagate in the guide. This minimum thickness is known as the cut-off thickness for the propagation of the mode at that wavelength ( $\lambda$ ). It can be calculated from the dispersion equation 1.14.<sup>38</sup> The expression is shown below:

$$h_{cut-off} = \frac{m\pi + \arctan\left(\frac{n_s^2 - n_c^2}{n_f^2 - n_s^2}\right)^{\frac{1}{2}}}{\frac{2\pi}{\lambda}(n_f^2 - n_s^2)^{\frac{1}{2}}} \quad (1.19)$$

#### 1.4. Types of laser resonators<sup>30,39,40</sup>

The simplest laser cavity consists of two mirrors facing each other, as shown in figure 1.1. There are other kinds of resonators that are frequently used in organic lasers (figure 1.5): planar microcavity, micro-ring resonator coated around an optical fiber, 1D or 2D distributed feedback resonators (DFB). The latter is equivalent to a 2D photonic crystal (PC).

A planar microcavity (figure 1.5.a) consists in an active film sandwiched between two mirrors, typically a commercial dielectric mirror and a thermally evaporated metal. Light propagates perpendicularly to the film plane, bouncing between the two mirrors. Although this architecture is easy to make, unfortunately, the distance traveled by the light during each pass through the gain region is small (<200 nm). Consequently, the lasing threshold is usually high.

An approach to make low-threshold lasers is to use a micro-ring resonator (figure 1.5.b). The easiest way to make such a resonator is to dip-coat a polymer film onto a glass optical fiber. In micro-ring resonators, light is totally internally reflected around the perimeter of the ring. Lasers of this type typically show narrow-linewidth lasing modes with spacing that varies inversely with the ring diameter. Single-mode lasing has been observed from rings with diameters of 5  $\mu\text{m}$ . Assuming that the round-trip losses are not substantially greater than in the case of planar microcavities, a much lower excitation density  $\sim 1 \mu\text{J}/\text{cm}^2$  is required in order to achieve sufficient gain to reach the lasing threshold. However, these resonators are distinctive in that they do not emit a well-defined directional output beam; instead, light is emitted uniformly in all radial directions.

When inorganic crystalline semiconductors are used to make waveguide lasers, mirrors are sometimes made simply by cleaving the crystal. The resulting facets at the ends of the waveguide reflect light because of the refractive index mismatch between the crystal and air. Unfortunately, organic lasers cannot be made so simply. The reflectivity at the film-air interfaces usually is less than 10% because the refractive index of organic materials is relatively low (1.6-2.0).

An alternative resonator to obtain low threshold and well-defined directional output beam in organic lasers, consists in a structure in which light is waveguided through large distances in the gain medium. An example of this kind of structure is the DFB laser which incorporates a periodic modulation of the refractive index so that light can



be reflected by Bragg scattering. Lasers of this type are different from most other types of lasers in that the mirrors are actually incorporated into the gain medium. If we compare DFBs structures with other resonant structures described, DFBs offer high reflectivities, longer gain lengths, and higher optical confinement of the oscillating mode, leading to very low operation thresholds. In some cases they have been so low that it was possible to pump with compact and cheap sources such as laser diodes or even LEDs. Besides, the emitted beam presents high quality and stability, allowing also output wavelength purity or single emission.<sup>41</sup>

In addition to the basic one dimensional (1D) DFB laser (figure 1.5c), there has been growing interest in recent years in more complicated diffractive resonators that may apply a 2D feedback in the plane of the active film. These structures are 2D DFB lasers also called a 2D PC (figure 1.5 d).

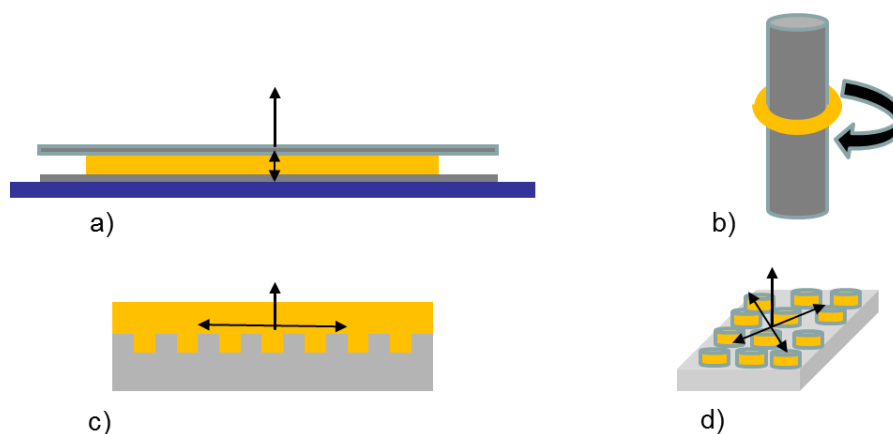


**Figure 1.5.-** Schematic resonators showing propagation directions of the resonant laser field: a) planar microcavity, b) micro-ring coated around an optical fiber, c) 1D DFB, d) 2D DFB or 2D PC.

### 1.5. Distributed feedback (DFB) lasers<sup>42-44</sup>

Among the different possible resonators used to make TFOLs, those in which the active film is in the form of a waveguide film, are the most interesting ones. DFB lasers have to date demonstrated the largest success. Besides the advantages explained in section 1.4, a DFB laser can be easily integrated with field-effect-transistor geometry, promising for the development of electrically-pumped TFOLs, and also it can be mechanically flexible if all layers in the devices are of organic nature.

The optical feedback and the out-coupling for the laser are achieved by the DFB resonator. In most cases it consists of a relief grating, patterned typically on a substrate on which the active material is coated (figure 1.6). The active film or gain medium works as a waveguide (explained in section 1.3), along which the light emitted

upon optical excitation propagates. The light feedback is produced by constructive interference (maximum coupling) of the waves coupled between forward and backward propagation along the waveguide.

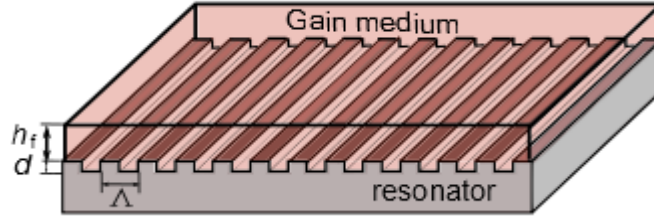


**Figure 1.6.-** DFB sketch.  $\Lambda$ : grating period,  $d$ : depth,  $h_f$ : film thickness.

In a 1D DFB laser, the resonant wavelength in the cavity satisfies the Bragg condition ( $\lambda_{\text{Bragg}}$ ) and is given by:

$$m \cdot \lambda_{\text{Bragg}} = 2 \cdot n_{\text{eff}} \Lambda \quad (1.20)$$

where  $m$  is the order of diffraction,  $n_{\text{eff}}$  is the effective refractive index of the waveguide, and  $\Lambda$  is the grating period.

In this work we are going to study second order DFB lasers ( $m=2$  in eq. (1.20)), for which light is coupled out of the film by first order diffraction, in a direction perpendicular to the waveguide film at a wavelength  $\lambda_{\text{DFB}}$  close to  $\lambda_{\text{Bragg}}$  (given by eq. 1.20). One advantage of using 1D gratings operating in the second order of diffraction,  $m=2$ , is that their properties are independent of the angle of the excitation beam over the sample and emission occurs in a perpendicular direction. This is an ideal situation if the DFB laser is envisaged to be used as a sensor. The  $n_{\text{eff}}$  value depends on  $h_f$ ,  $\lambda$ ,  $n_f$ ,  $n_s$ ,  $n_c$ , (see eq. 1.18).

An important characteristic of the presence of the periodic structure is the existence of a range of wavelengths forbidden to propagate in any direction. In this sense, the wavelength that exactly satisfies the Bragg condition ( $\lambda_{\text{Bragg}}$  in eq. 1.20) cannot propagate in the waveguide. This is known as the photonic stopband. Coupled mode theory<sup>45</sup> predicts that the DFB laser will normally oscillate on a pair of wavelengths, one at either edge of the photonic stopband. The stopband is translated in the observation of a characteristic dip in the emission intensity due to the inhibition of the propagation of waveguided photons by the gratings.<sup>39,41</sup> In the second order DFB ( $m = 2$ ) there is a strong discrimination between the two band-edge modes, caused by their different radiation losses and coupling strengths to free space radiation, so only the mode at the long wavelength side of the Bragg dip is observed. For this reason it is often said that these lasers show band-edge emission.

DFB grating fabrication is generally accomplished by techniques such as electron beam lithography (EBL), holographic lithography (HL), nanograting transfer or nanoimprint lithography (NIL).<sup>9</sup> HL and NIL will be explained in section 4.1.3 since they have been used to prepare the DFB gratings in this thesis. While NIL shows the highest potential for fabrication scalable to mass production, HL allows the preparation of large size devices (various cm) and provides great feasibility for changing the grating period ( $\Lambda$ ) without the need of changing the stamp master, and therefore, tuning easily the emission wavelength of the device. The stamp master (used in NIL) is prepared by other methods, generally expensive (often EBL).

In this thesis we have prepared devices with different types of DFB geometries, in particular geometries I, III and IV of figure 1.7. Geometry II, also shown in the figure, has been used in previous works of the group.

- (I) Grating on inorganic substrate (i.e. transparent fused silica, silicon oxidized at the surface ( $\text{SiO}_2$ ) of a silicon wafer or glass) fabricated by EBL, NIL<sup>43,46,47</sup> or HL<sup>48</sup> and subsequent etching; active film on top of it. This is the most common resonator used in the literature. The resonator can be reused in different devices after dissolving the active film and depositing a new one. Lasers with this kind of DFB geometry are the ones showing generally the lowest thresholds.<sup>49</sup>
- (II) Grating on active film fabricated by NIL. The advantage of this geometry with respect to geometry I it is that fabrication is simpler because no etching methods to transfer the pattern to the substrate are needed.<sup>50</sup>
- (III) Grating on resist layer, fabricated by HL<sup>51-53</sup> or NIL, deposited over inorganic substrate and active film on top of it. Also in this case the etching step is not needed. However, due to the small difference in the refractive indexes of resist and the active film, thresholds are generally higher.
- (IV) Grating on photoresist layer, fabricated by HL, deposited over the active film. In this case the active material thickness is uniform. This type of geometry has been used for the first time in the frame of this thesis. As we will show later, a remarkable aspect is that their performance is as good as that of lasers based on geometry I.

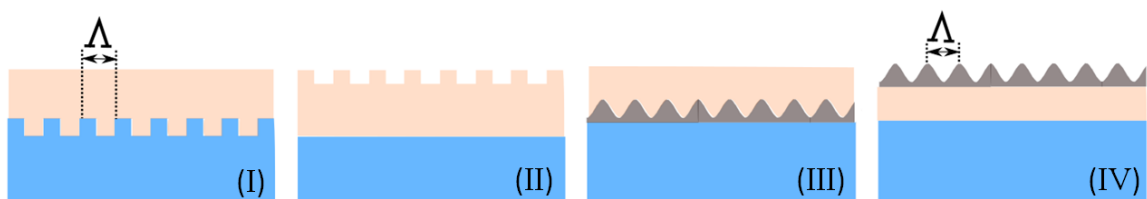


**Figure 1.7.-** Different types of DFB device geometries. Grating period, ( $\Lambda$ ).